Письма в ЖЭТФ, том 80, вып. 2, с. 75 – 80

The role of finite kinematic bounds in the induced gluon emission from fast quarks in a finite size quark-gluon plasma

B. G. Zakharov

L. D. Landau Institute for Theoretical Physics RAS, 117334 Moscow, Russia

Поступила в редакцию 7 June 2004

We study the influence of finite kinematic boundaries on the induced gluon radiation from a fast quark in a finite size quark-gluon plasma. The calculations are carried out for fixed and running coupling constant. We find that for running coupling constant the kinematic correction to the radiative energy loss is small for quark energy $\gtrsim 5\,\mathrm{GeV}$. Our results differ both analytically and numerically from that obtained by the GLV group [6]. The effect of the kinematic cut-offs is considerably smaller than reported in [6].

PACS: 12.38.Mh

1. It is very likely that parton energy loss due to the induced gluon radiation caused by multiple scattering [1 – 7] plays a major role in suppression of high-p_T hadron spectra in heavy-ion collisions observed at RHIC [8, 9]. There is an attractive idea [10] to use this phenomenon (usually called "jet-quenching") to obtain information about the density of hot quark-gluon plasma (QGP) produced in AA-collisions. Such a jet tomographic analysis requires accurate methods for evaluating the induced gluon emission. In recent years this problem has been attacked from several directions. In [3] (see also [11 – 13]) we have developed a light-cone path integral (LCPI) approach to the induced radiation. The induced gluon spectrum was expressed through a solution of a two-dimensional Schrödinger equation in the impact parameter space with an imaginary potential. This approach accounts for the Landau-Pomeranchuk-Migdal (LPM) effect [14, 15], finite-size and mass effects which are important for the QGP produced in AA-collisions. In [2, 5] the radiative energy loss was addressed using diagrammatic formalism. Similarly to the LCPI approach the BDMPS approach [2, 5] expresses the gluon spectrum through a solution of a two-dimensional Schrödinger equation in the impact parameter space. However, the BDMPS formalism applies only in the limit of strong LPM suppression. In this regime it is equivalent [5, 13] to the approach [3]. The GLV group [6] has developed within the soft gluon approximation an approach in momentum space which applies to thin plasmas when the mean number, $\bar{N}$, of jet scatterings is small, and performed calculations accounting for the $N = 1, 2, 3$ rescatterings.

For applications of the formalisms [3, 5, 6] to the tomographic analysis of experimental data on AA-collisions it is important to understand the limits of applicability of these approaches. In the analyses [3, 5, 6] the QGP is modeled by a system of Debye screened color centers [1], and parton scattering is treated in the small-angle approximation. The LCPI [3] and BDMPS [2, 5] approaches, formulated in the impact parameter space, in addition, imply that the integration over the transverse momenta can be extended up to infinity ignoring finite kinematic boundaries. The small-angle approximation for fast partons moving through the medium should work well for parton energy $E \gg \mu_D$, where μ_D is the Debye screening mass which plays the role of a natural infrared cut-off and energy scale for parton scatterings in the QGP. For RHIC and LHC conditions, where $\mu_D \sim 0.5\,\mathrm{GeV}$ [16], it means $E \gtrsim 3 \div 5\,\mathrm{GeV}$. It is however not clear whether the approximation of static color centers neglecting recoil effects is adequate for $E \sim 5\,\mathrm{GeV}$. For such energies the kinematic constraints on the momentum transfer $q \lesssim q_{\max} \sim \sqrt{EE_{th}}$, where $E_{th} \approx 3T$ is the typical thermal energy of quarks and gluons in the QGP, may be important. The GLV group [6] has reported that the kinematic cut-offs suppress greatly the parton energy loss, ΔE. Even at $E \sim 1000\,\mu_D$ for the leading $N = 1$ contribution to ΔE for a homogeneous QGP with thickness $L \approx 5\,\mathrm{fm}$ the authors have found the suppression ~ 0.5, and for $E \sim 10\,\mu_D$ they give the suppression ~ 0.16.

The approaches [3, 5] become inapplicable when the kinematic bounds become important. The GLV formalism [6], which does not treat accurately parton scattering near the kinematic limit, also cannot be used for quantitative calculations in this regime. Thus, if the kinematic effect were as strong as found in [6], the available approaches to the induced radiation would be inapplicable even at LHC energies. For this reason the kinematic effect merits further investigations. In particular, it is clearly desirable to study the effect of the running coupling constant. The decrease of the coupling constant near the kinematic bounds should act as a natural cut-off of large parton transverse momenta and diminish the role of the recoil effects. Another remaining open question is related to the different cut-offs for the initial and final partons. The authors of [6] have used for scattering of the radiated gluon the same cut-off in the momentum transfer as that for the initial parton. However, for soft gluons with $x \ll 1$ (hereafter x is the gluon fractional momentum) the $q_{\max}$ is considerably smaller than for the initial parton. In the present paper we address the role of the kinematic cut-offs accounting for the running coupling constant and different cut-offs for the initial and final partons. The analysis is performed for the $N=1$ scattering which dominates the induced spectrum for RHIC and LHC conditions. We find that although the difference in the initial and final state cut-offs changes the analytical form of the induced spectrum, numerically the effect is insignificant. For fixed coupling constant the kinematic corrections become important for $E \lesssim 10 \div 20\,\mathrm{GeV}$, and for running one the kinematic effect is small even at $E \sim 5\,\mathrm{GeV}$. We find that the kinematic effect is considerably smaller than found in [6].

2. We consider a fast quark with energy E produced at $z=0$ (we choose the z-axis along the momentum of the quark) traversing a medium of thickness L, which eventually splits into a gluon and final quark with the energies xE and $(1-x)E$ respectively. We assume that parton energies are much larger than the thermal quasiparticle masses in the QGP. The $N=1$ induced spectrum can be represented in the form

$$\frac{dP}{dx} = \int\limits_0^L dz\, n(z) \frac{d\sigma^{BH}(x,z)}{dx}, \qquad (1)$$

where $n(z)$ is the number density of the medium (the summation over the triplet (quark-antiquark) and octet (gluon) color states is implied on the right-hand side of (1)), and $d\sigma^{BH}(x,z)/dx$ is the in-medium (z-dependent) Bethe-Heitler cross section. It can be written as

$$\frac{d\sigma^{BH}(x,z)}{dx} = J_{bb} + J_{cc} + J_{dd} + 2J_{bc} + 2J_{cd} + \\ + 2J_{db} + 2J_{ae} + 2J_{af} + 2J_{ag} + 2J_{ah}, \qquad (2)$$

with $J_{\alpha\beta}$ given by

$$J_{\alpha\beta} = \frac{E}{(2\pi)^5} \mathrm{Re} \int d\mathbf{q} d\mathbf{p} T_\alpha(\mathbf{q},\mathbf{p}) T^*_\beta(\mathbf{q},\mathbf{p}), \qquad (3)$$

where the amplitudes T_α diagrammatically are shown in Fig.1, $\mathbf{q}$ and $\mathbf{p}$ are the transverse momenta of the t-channel and emitted gluons, respectively. Note

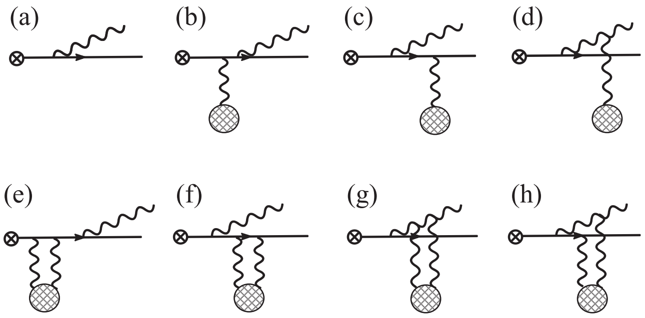

Fig.1. The set of the Feynman diagrams for the $N=1$ contribution to the induced gluon spectrum

that the interference between the double-gluon exchange diagrams (e), (f), (g), (h) and the diagram without gluon exchange (a) is important to ensure unitarity.

The diagrams of Fig.1 can be evaluated with the help of the ordinary perturbative formula

$$T = \int\limits_0^\infty dz' \int d\boldsymbol{\rho} g \bar{\psi}_f(\boldsymbol{\rho},z') \gamma^\mu A_\mu(\boldsymbol{\rho},z') \psi_i(\boldsymbol{\rho},z'), \qquad (4)$$

where $\boldsymbol{\rho}$ is the transverse coordinate, $\psi_{i,f}(\boldsymbol{\rho},z')$ are the wave functions of the initial and final quarks, and $A_\mu(\boldsymbol{\rho},z')$ is the wave function of the emitted gluon (hereafter we omit the color factors and spin indices). In (4) we do not explicitly indicate the dependence of the wave functions on the position of the scattering center. The quark wave functions using the light-cone spinor basis can be written as

$$\psi_j(\boldsymbol{\rho},z') = \exp(iE_j z') \hat{U}_j \phi_j(\boldsymbol{\rho},z'), \qquad (5)$$

where the operator $\widehat{U}_j$ reads

$$\widehat{U}_j = \left(1 + \frac{\boldsymbol{\alpha}\mathbf{p} + \beta m_q}{2E_j}\right) \chi_j. \qquad (6)$$

Here χ_j is the quark spinor (normalized to unity), $\boldsymbol{\alpha} = \gamma^0 \boldsymbol{\gamma}$, $\beta = \gamma^0$, and $\mathbf{p} = -i\nabla_\perp$. The transverse wave function $\phi_j(\boldsymbol{\rho},z')$ entering (5) is governed by the two-dimensional Schrödinger equation in which z' plays the role of time

$$i\frac{\partial \phi_j(\boldsymbol{\rho},z')}{\partial z'} = \left[\frac{(\mathbf{p}^2 + m_q^2)}{2E_j} + v(\boldsymbol{\rho},z')\right] \phi_j(\boldsymbol{\rho},z'), \qquad (7)$$

where

$$v(\boldsymbol{\rho}, z') = \delta(z'-z)\int \frac{d\mathbf{q}}{(2\pi)^2}\exp(i\mathbf{q}\boldsymbol{\rho})v(\mathbf{q}),$$
$$v(\mathbf{q}) = \frac{4\pi\alpha_s(q)}{\mathbf{q}^2+\mu_D^2}, \qquad (8)$$

is the potential generated by the one-gluon exchange between quark and the Debye screened color center. In the longitudinal direction we treat the potential as a point-like. In the same form one can represent the gluon wave function (up to an obvious change of the spin operator and color factors).

The amplitudes entering (3) can be easily obtained from (4) treating in (7) the potential v as a perturbation. For the diagrams with gluon exchanges in the z' regions $0 < z' < z$ and $z' > z$ the transverse wave functions age given by the plane waves (with different transverse momenta in these two regions of z')

$$\phi_j(\boldsymbol{\rho}, z') \propto \exp\left\{i\left[\mathbf{p}_j\boldsymbol{\rho} - z'\frac{(\mathbf{p}_j^2+m_j^2)}{2E_j}\right]\right\}. \qquad (9)$$

The color center acts as a kick which changes the quark (or gluon) transverse momentum at $z' = z$. The corresponding amplitude $\propto v(\mathbf{q})$ for one-gluon exchange diagrams, and $\propto \int d\mathbf{p}v(\mathbf{p})v(\mathbf{q}-\mathbf{p})$ for the double-gluon exchange ones. Note that, eventually, the $\boldsymbol{\rho}$-integration in (4) ensures conservation of the transverse momentum.

To account for the kinematic boundaries we introduce in the amplitudes the cut-off factors. For each t-channel gluon we modify the propagator introducing the cut-off factor $\theta(q_{\max}-q)$. Here $q_{\max}$ is the upper kinematic bound on the momentum transfer for the parton to which the t-channel gluon is attached. Also, we modify the qqg-vertex for splitting the initial fast quark into quark-gluon system introducing the cut-off factor $\theta(k_{\max}-k)$, k is the transverse momentum of the gluon in the frame where the total transverse momentum of the quark-gluon state equals zero, and $k_{\max} = E\min(x, 1-x)$ (here E is the initial quark energy). The above prescription ensures that parton scattering angles are small, and the momentum transfer does not exceed the kinematic bounds.

Using (2)–(8) after straightforward but a bit cumbersome calculations the effective Bethe-Heitler cross section can be represented in the form

$$\frac{d\sigma^{BH}(x,z)}{dx} = \frac{d\sigma_1^{BH}(x,z)}{dx} + \frac{d\sigma_2^{BH}(x,z)}{dx}, \qquad (10)$$

where

$$\frac{d\sigma_1^{BH}(x,z)}{dx} = \frac{2C_T}{\pi^2 x}\left(1-x+\frac{x^2}{2}\right)\times$$
$$\times\int d\mathbf{q}d\mathbf{k}\frac{\alpha_s^2(q)}{(\mathbf{q}^2+\mu_D^2)^2}\Big[\theta(q_3-q)F(\mathbf{k},\mathbf{q},z) +$$
$$+\theta(q_1-q)F(\mathbf{k},\mathbf{q}(1-x),z) -$$
$$-\frac{1}{N_c^2}\theta(q_2-q)F(\mathbf{k},\mathbf{q}x,z)\Big], \qquad (11)$$

$$F(\mathbf{k},\mathbf{q},z) =$$
$$= \left[\frac{\mathbf{k}^2\Theta^2(\mathbf{k})}{(\mathbf{k}^2+\epsilon^2)^2} - \frac{(\mathbf{k}-\mathbf{q})\mathbf{k}\Theta(\mathbf{k})\Theta(\mathbf{k}-\mathbf{q})}{(\mathbf{k}^2+\epsilon^2)((\mathbf{k}-\mathbf{q})^2+\epsilon^2)}\right]\times$$
$$\times\left[1-\cos\left(\frac{iz}{l(\mathbf{k},x)}\right)\right], \qquad (12)$$

$$\frac{d\sigma_2^{BH}(x,z)}{dx} = \frac{2C_T}{C_A\pi^2 x}\left(1-x+\frac{x^2}{2}\right)\times$$
$$\times\int d\mathbf{q}\frac{\alpha_s^2(q)}{(\mathbf{q}^2+\mu_D^2)^2}[C_F(\theta(q_0-q)-\theta(q_2-q)) +$$
$$+C_A(\theta(q_2-q)-\theta(q_3-q))]\times$$
$$\times\int d\mathbf{k}\frac{\mathbf{k}^2\Theta^2(\mathbf{k})}{(\mathbf{k}^2+\epsilon^2)^2}\left[1-\cos\left(\frac{iz}{l(\mathbf{k},x)}\right)\right], \qquad (13)$$

with the following shorthands:

$$l(\mathbf{k},x) = \frac{2Ex(1-x)}{\mathbf{k}^2+\epsilon^2}, \qquad (14)$$

$$q_0 = q_{\max}(E), \quad q_1 = q_{\max}(Ex),$$
$$q_2 = q_{\max}(E(1-x)), \quad q_3 = \min(q_1, q_2), \qquad (15)$$

$\Theta(\mathbf{k}) = \sqrt{\alpha_s(k)}\theta(k_{\max}-k)$, $\epsilon^2 = m_q^2x^2 + m_g^2(1-x)$, $m_{q,g}$ are the thermal quark and gluon quasiparticle masses, $C_{T,F,A}$ are the color Casimir factors of the color center, quark and gluon respectively. Eq.(15) corresponds to the above described scheme when each scattered parton has its own q-cut-off factor. Note that in the soft gluon limit $x \ll 1$ our formulas do not reduce to that of Ref. [6]. If one uses for the final partons the same $q_{\max}$ as for the initial quark as was done in [6], the second term on the right-hand side of (10) vanishes. This term emerges inevitably because the initial and final partons have different phase space for their scattering. Below for comparison with [6] we also present the results for $q_i = q_{\max}(E)$ as in [6].

The quantity $L_f = l(\mathbf{k}=0, x)$ characterizes the longitudinal scale of gluon emission, i.e., the gluon formation length. The induced spectrum depends crucially on the ratio L_f/L [3, 4, 17]. For gluons with small formation length $L_f \ll L$ the finite-size effects caused by the oscillating cosine on the right-hand side of (12), (13) becomes small. In this regime the rapidly oscillating cosine can be neglected, and the effective cross section (10) becomes equal to the ordinary Bethe-Heitler one, i.e., to the cross section for a quark which approaches the color center from outside. In contrast, when $L_f \gtrsim L$ the finite size effects due to the cosine in (12), (13) suppress greatly the radiation rate as compared to the Bethe-Heitler one [4, 17]. This suppression, physically, is connected with small transverse size of the qg system (it is $\propto L$). In this regime the t-channel gluons cannot distinguish the $|q\rangle$ and $|qg\rangle$ Fock components of the physical quark and for this reason the gluon emission turns out to be suppressed. One remark regarding the Bethe-Heitler regime for $L_f \ll L$ is in order here. Diagrammatically, the ordinary Bethe-Heitler cross section is given by the diagrams (b), (c), (d) of Fig.1 involving only one-gluon exchange. However, our formulas include the interference between the diagram (a) and (e), (f), (g), (h). The explanation of this fact is as follows. For a quark incident on the color center from outside the amplitudes (b), (c), (d) should be evaluated integrating over z' in (4) from $-\infty$ (with usual adiabatic switching off of the coupling constant for $|z'| \to \infty$). For a quark produced in a hard reaction at $z' = 0$ the z'-integration region is $(0, \infty)$. This gives rise to additional endpoint terms (corresponding to $z' = 0$) in the cross section which are absent when the lower limit equals $-\infty$. However, similar endpoint terms emerge for the interference term involving the double-gluon exchange diagrams as well. They cancel exactly the endpoint terms stemming from the graph (b), (c), (d). As a result for $z \to \infty$ our effective cross section (10) equals the ordinary Bethe-Heitler one.

It should be noted that our method (and any other one based on the GW model [1] for the QGP) can only give an estimate for the kinematic correction. It is inapplicable in the regime of strong kinematic suppression when the spectrum becomes very sensitive to the detailed form of the kinematic cut-offs. This fact is closely connected with the anti-leading log character of the $\mathbf{q}, \mathbf{k}$-integrations in (11). Contrary to the ordinary leading log situation, say, in $\gamma^* \to q\bar{q}$ transition in deep inelastic scattering, where the typical values of the momentum transfer q is smaller than the internal momentum k, in the case of the induced gluon emission in the high energy limit when $L_f \gg L$ the dominating contribution to the induced spectrum comes from $q \gtrsim k$. A detailed discussion of this phenomenon is given in [17].

The effective Bethe-Heitler cross section evaluated without kinematic cut-offs, i.e., with $q_i = k_{\max} = \infty$, is given by the first term on the right-hand side of (10). After the Fourier transform it can be represented in the impact parameter space in the form obtained previously [18, 17] within the LCPI formalism

$$\frac{d\sigma^{BH}(x,z)}{dx} = \mathrm{Re} \int d\boldsymbol{\rho}\, \Psi^*(\boldsymbol{\rho}, x)\sigma_3(\rho, x)\Psi_m(\boldsymbol{\rho}, x, z)\,, \tag{16}$$

where $\Psi(\boldsymbol{\rho}, x)$ is the ordinary light-cone wave function for the $q \to gq$ transition in vacuum, $\Psi_m(\boldsymbol{\rho}, x, z)$ is the z-dependent light-cone wave function describing the quark-gluon Fock component at the longitudinal coordinate z, and $\sigma_3(\rho, x)$ is the three-body cross section of a $q\bar{q}g$ system with a particle in the medium (the explicit form of the wave functions and three-body cross section can be found in [17]). In the $q\bar{q}g$ system antiquark is located (in the transverse space) in the center of mass of the qg pair, and the relative separations satisfies the relation $(\boldsymbol{\rho}_g - \boldsymbol{\rho}_{\bar{q}})x = (1-x)(\boldsymbol{\rho}_{\bar{q}} - \boldsymbol{\rho}_q)$.

3. We have performed numerical calculations for fixed and running coupling constant. In the first case we take $\alpha_s = 0.5$ [19]. For running coupling constant we use the one-loop formula with $\Lambda_{\mathrm{QCD}} = 0.3$ GeV frozen at the value $\alpha_s = 0.65$. In this case α_s approximately satisfies the relation

$$\int\limits_0^{2\,\mathrm{GeV}} dk \frac{\alpha_s(k)}{\pi} \approx 0.36 \text{ GeV} \tag{17}$$

obtained from the analysis of the heavy quark energy loss [20]. We have carried out the calculations for expanding plasma. We use the Bjorken [21] model with $T\tau^3 = T_0\tau_0^3$, and take the initial conditions suggested in [22] for heavy ion central collisions at RHIC: $T_0 = 446\,\mathrm{MeV}$ and $\tau_0 = 0.147\,\mathrm{fm}$. For the upper limit of the z-integration in (1) we take $L = R_A \approx 6\,\mathrm{fm}$. For quark and gluon quasiparticle masses we use the values obtained in [16] from the lattice data $m_q \approx 0.3$ and $m_g \approx 0.4\,\mathrm{GeV}$. With the above value of m_g from the perturbative relation $\mu_D = \sqrt{2}m_g$ one obtains for the Debye screening mass $\mu_D \approx 0.57\,\mathrm{GeV}$. For the energy dependence of the maximum momentum transfer we take $q^2_{\max}(E) \approx E\bar{E}_{th}$ with $\bar{E}_{th} = 750\,\mathrm{MeV}$. It is smaller than $q^2_{\max}(E) \approx 3E\mu_D$ used in [6].

In Figs.2, 3 we plot the induced gluon spectrum for $E = 5$, 10 and 20 GeV evaluated using (1), (10)–(15) with (solid line) and without (dashed line) the kinematic cut-offs for fixed and running α_s. The results with kinematic cut-offs have been obtained for q_i given in (15). For this version we also plot the spectrum without

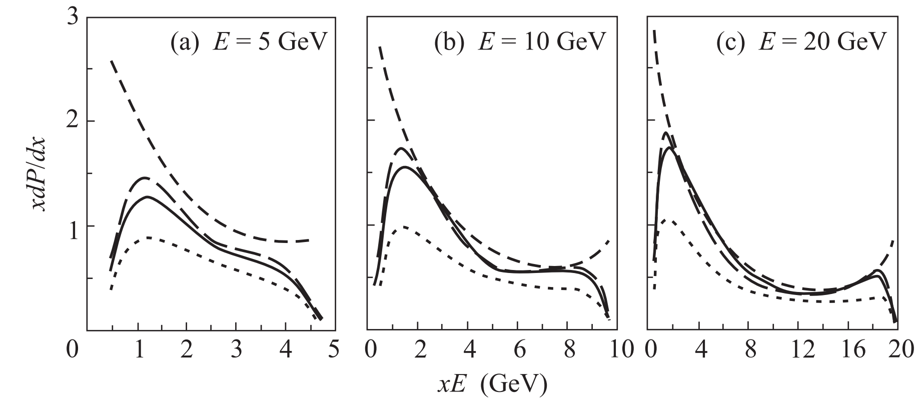

Fig.2. The spectrum of the induced $q \to gq$ transition versus the gluon energy xE for RHIC conditions for fixed coupling constant. The solid lines are for q_i given in (15) and the long-dashed lines are for the same q-cut-offs for the initial and final partons with $q_i = q_{\max}(E)$. The dashed lines show the spectrum obtained without kinematics cut-offs. The spectrum without the second term in (10) for q_i given in (15) is shown by the dotted curves

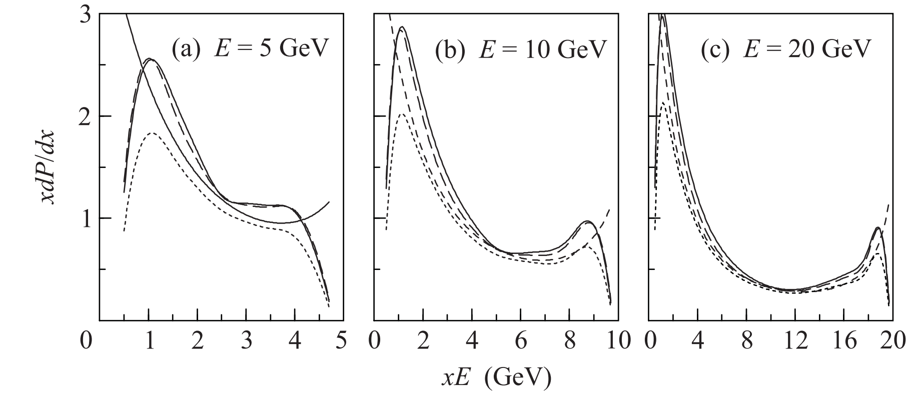

Fig.3. The same as in Fig. 2 but for running coupling constant.

the second term in (10) (dotted line). In Figs.2, 3 we also show the results for the same kinematic cut-offs for initial and final partons obtained with $q_i = q_{\max}(E)$ (long-dashed line). From Figs.2, 3 one sees that the kinematic cut-offs become especially important when the energy of the radiated gluon (or the final quark) $\lesssim 1 \div 2\,\mathrm{GeV}$. The kinematic correction is smaller for running coupling constant. It is also seen that for fixed coupling constant the relative contribution from the second term in (10) is larger. It is natural since for the running α_s the contribution from large transverse momenta is suppressed. The total spectrum in the above two scheme of the q-cut-off turns out to be approximately the same.

To illustrate the effect of the kinematic cut-offs on the quark energy loss in Fig.4 we plot the energy dependence of the kinematic K-factor

$$K(E) = \frac{\Delta E_{f.b.}}{\Delta E_{i.b.}}, \tag{18}$$

where $\Delta E_{f.b.}$ and $\Delta E_{i.b.}$ are the quark energy losses evaluated with (for q_i as given in (15)) and without kinematic constraints, respectively. We define ΔE as

$$\Delta E = E \int\limits_{x_{\min}}^{x_{\max}} dx x \frac{dP}{dx} \tag{19}$$

with $x_{\min} = m_g/E$, $x_{\max} = 1 - m_q/E$. Fig.4 demonstrates that for fixed coupling constant the kinematic cut-offs are important for $E \lesssim 20$ GeV. For running coupling the kinematic correction is small even for $E \sim 5$ GeV. One can see that the difference between the cut-offs given in (15) (thick curves) and $q_i = q_{\max}(E)$ (thin curves) is less than $\sim 10\%$.

The kinematic K-factor shown in Fig. 4 is obtained for an expanding plasma with $n(z) \propto 1/z$. For comparison with the analysis [6] we have also carried out calculations for a homogeneous plasma. In this case the kinematic effect is weaker since the relative contribution of the region of small z where the typical

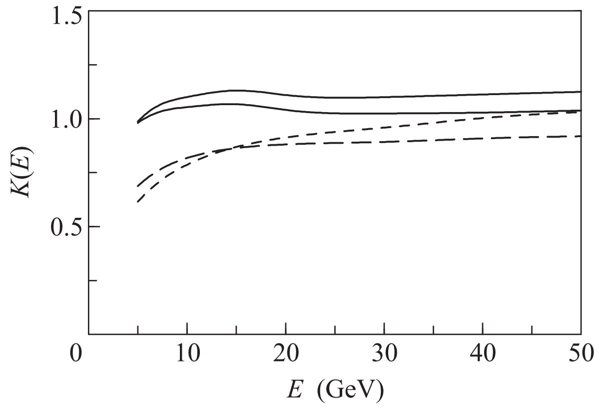

Fig.4. The energy dependence of the kinematic K-factor (18) for RHIC conditions for running (solid line) and fixed (dashed line) coupling constant. The thick lines are for the q-cut-off given in (15) and the thin lines are for $q_i = q_{\max}(E)$

parton transverse momenta are large (they are $\propto 1/\sqrt{z}$) is smaller. For correspondence with [6] we have taken $q_{\max}^2 = 3E\mu_D$ (the same for the initial and final partons) and $k_{\max}^2 = 4E^2 \min(x^2, x(1-x))$ used in [6] which give somewhat smaller kinematic effect than our cut-offs. We have obtained a small kinematic effect, say, $K \approx 0.9$ at $E = 5\,\text{GeV}$ and $K \approx 0.94$ at $E = 10\,\text{GeV}$ (we have used fixed coupling constant as in [6]). It is considerably larger than the suppression reported in [6] ($\sim 1/6$ for $E = 5\,\text{GeV}$). In connection with strong kinematic suppression reported in [6] we would like to emphasize one more time that within the approximation of static color centers [1] when the kinematic cut-offs are introduced by hand the regime of strong kinematic effect cannot be described accurately. It is clear that the analysis of the induced radiation in this regime requires an accurate treatment of the recoil effects. In this case the fast partons moving through QGP and partons from QGP should be treated on an even footing. Note also that in this regime suppression of the radiative energy loss may largely be compensated by the collisional energy loss due to strong recoil effects.

In summary, the form of the induced gluon spectrum obtained in the present analysis shows that the kinematic effect is relatively small and is mainly important near to the endpoints $x \sim 0$ and $x \sim 1$ when the energy of the radiated gluon (or of the final quark) is about $\sim 2 \div 3$ units of the Debye screening mass, i.e., about $1 \div 2\,\text{GeV}$ for RHIC and LHC conditions. For fixed coupling constant the kinematic correction to the quark energy loss becomes small for $E \gtrsim 20\,\text{GeV}$, for running coupling constant it is small even at $E \sim 5\,\text{GeV}$. The kinematic effect found in our analyses is considerably smaller than reported in [6]. Our results say that in the region of the gluon fractional momentum $\delta \lesssim x \lesssim 1 - \delta$ ($\delta \sim (2 \div 3)\mu_D/E$), the induced spectrum can be evaluated to reasonable accuracy within the LCPI approach [3] which ignores the kinematic bounds. This approach can be used for evaluation of the energy loss and nuclear suppression factor [19] for RHIC and LHC energies.

I thank N. N. Nikolaev for discussion of the results. I am grateful to the High Energy Group of the ICTP for the kind hospitality during my visit to Trieste where the present calculations were carried out.

1. M. Gyulassy and X.-N. Wang, Nucl. Phys. **B420**, 583 (1994); X.-N. Wang, M. Gyulassy, and M. Plumer, Phys. Rev. **D51**, 3436 (1995).
2. R. Baier, Y. L. Dokshitzer, A. H. Mueller et al., Nucl. Phys. **B483**, 291 (1997); ibid. **B484**, 265 (1997).
3. B. G. Zakharov, JETP Lett. **63**, 952 (1996).
4. B. G. Zakharov, JETP Lett. **65**, 615 (1997).
5. R. Baier, Y. L. Dokshitzer, A. H. Mueller, and D. Schiff, Nucl. Phys. **B531**, 403 (1998).
6. M. Gyulassy, P. Lévai, and I. Vitev, Nucl. Phys. **B594**, 371 (2001).
7. U. A. Wiedemann, Nucl. Phys. **A690**, 731 (2001).
8. G. David et al. (PHENIX Coll.), Nucl. Phys. **A698**, 227 (2002); D. d'Enterria et al. (PHENIX Coll.), Nucl. Phys. **A715**, 749 (2003).
9. J. C. Danlop et al. (STAR Coll.), Nucl. Phys. **A698**, 515 (2002); J. C. Klay et al. (STAR Coll.), Nucl. Phys. **A715**, 733 (2003).
10. M. Gyulassy, P. Lévai, and I. Vitev, Phys. Lett. **B538**, 282 (2002).
11. B. G. Zakharov, Phys. Atom. Nucl. **61**, 838 (1998).
12. B. G. Zakharov, JETP Lett. **70**, 176 (1999).
13. R. Baier, D. Schiff, and B. G. Zakharov, Ann. Rev. Nucl. Part. **50**, 37 (2000).
14. L. D. Landau and I. Ya. Pomeranchuk, Dokl. Akad. Nauk SSSR **92**, 535, 735 (1953).
15. A. B. Migdal, Phys. Rev. **103**, 1811 (1956).
16. P. Lévai and U. Heinz, Phys. Rev. **C57**, 1879 (1998).
17. B. G. Zakharov, JETP Lett. **73**, 49 (2001).
18. B. G. Zakharov, Proc. of the at 33rd Rencontres de Moriond: QCD and High Energy Hadronic Interactions, Ed. J. Tran Thanh Van, Les Arcs, France, 21-28 Mar 1998, p. 533; hep-ph/9807396.
19. R. Baier, Yu. L. Dokshitzer, A. H. Mueller, and D. Schiff, JHEP **0109**, 033 (2001); hep-ph/0106347 (2001).
20. Yu. L. Dokshitzer, V. A. Khoze, and S. I. Troyan, Phys. Rev. **D53**, 89 (1996).
21. J. D. Bjorken, Phys. Rev. **D27**, 140 (1983).
22. R. J. Fries, B. Müller, and D. K. Srivastava, nucl-th/0208001 (2003).